

New europium coordination polymers with efficient energy transfer from conjugated tetracarboxylate ligands to Eu^{3+} ion: syntheses, structures, luminescence and magnetic properties†

Li-Feng Wang,^{a,b} Ling-Chen Kang,^a Wen-Wei Zhang,^{*a} Fang-Ming Wang,^a Xiao-Ming Ren^{*b} and Qing-Jin Meng^a

Received 18th April 2011, Accepted 29th June 2011

DOI: 10.1039/c1dt10693g

Two novel lanthanide coordination polymers, $[\text{Eu}_2(\text{EBTC})(\text{DMF})_5(\text{NO}_3)_2] \cdot \text{DMF}$ (**1**) and $[\text{Eu}_2(\text{BBTC})_{1.5}(\text{CH}_3\text{OH})_2(\text{H}_2\text{O})_2] \cdot 7\text{DMF} \cdot \text{HNO}_3$ (**2**) (EBTC⁴⁻ = 1,1'-ethynebenzene-3,3',5,5'-tetracarboxylate; BBTC⁴⁻ = 1,1'-butadiynebenzene-3,3',5,5'-tetracarboxylate), were successfully synthesized from conjugated ligands of EBTC⁴⁻ and BBTC⁴⁻. Although the two tetracarboxylate ligands have similar structures, their different rigidity/flexibility results in quite different networks upon complexation. Complex **1** has a two-dimensional (2-D) layered structure with two crystallographically independent Eu^{3+} ions, one in a distorted monocapped square-antiprism and the other in a distorted square-antiprism coordination geometry. Complex **2** exhibits a three-dimensional (3-D) porous framework, with one type of Eu^{3+} in a distorted square-antiprism and the other in a trigondodecahedron environment. Both **1** and **2** emit the intensely red characteristic luminescence of Eu^{3+} ion at room temperature, with a long lifetime of up to 1.3 and 0.7 ms, respectively, during which the ligand emission of EBTC⁴⁻/BBTC⁴⁻ was quenched by the Eu^{3+} ion, indicating the existence of efficient energy transfer between the conjugated ligand of EBTC⁴⁻/BBTC⁴⁻ and the Eu^{3+} ion. Thus, both EBTC⁴⁻ and BBTC⁴⁻ are ideal ligands with an “antenna” effect for the Eu^{3+} ion. The two complexes show the single-ion magnetic behaviors of Eu^{3+} with strong spin–orbit coupling interactions even if there are shorter distances (5.714 Å for **1** versus 4.275 and 5.360 Å for **2**) between the neighboring Eu^{3+} ions connected by oxygen atoms of the tetracarboxylates.

Introduction

Lanthanide coordination compounds have appealing luminescence¹ and/or magnetic properties,² and these technologically important properties make them have potential applications in sensors, optical storage, and lighting devices.³ Lanthanoid ions, such as Eu^{3+} and Tb^{3+} , show very narrow spectral bands, thus providing the high chromatic purity that is very important for some practical technical applications. However, the absorption and fluorescence of these ions are very low since the electronic transitions are forbidden by parity (Laporte) selection rules. Fortunately, the intensely characteristic emission of lanthanide

ions can be achieved *via* ligating an organic compound as an “antenna” for energy transfer to lanthanide ions.⁴ Alternatively, the magnetic properties of lanthanide ions are also fascinating, and the strongly unquenched f orbital angular momentum makes the lanthanide coordination compounds exhibit a pronounced magnetic anisotropy.^{2e,5}

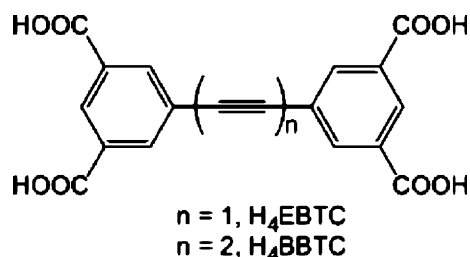
Nowadays, a particular class of materials, known as metal–organic frameworks (MOFs) or coordination polymers containing Ln^{3+} ions (LnMOFs), constitute a robust platform for the creation of various types of multifunctional materials. LnMOFs, combining light emission with microporosity, magnetism, catalysis, chirality, ion exchange and molecular separation properties, present a unique chance of observing synergistic effects, which assists in defining targets and directing future research.⁶ An ideal “antenna” ligand for lanthanide ions should have intense UV absorption and the energy level of its T_1 should be matched, namely close to, but just higher than, the resonance level of lanthanide ions, and usually the conjugated organic molecules are good candidates for “antenna” ligands of lanthanide ions. In addition, lanthanide ions favor binding to atoms that can act as hard Lewis bases (such as oxygen atoms). Taking into account the facts above, we designed and synthesized

^aState Key Laboratory of Coordination Chemistry, School of Chemistry and Chemical Engineering, Nanjing University, Nanjing 210093. Email: wwzhang@nju.edu.cn

^bDepartment of Applied Chemistry, College of Science, Nanjing University of Technology, Nanjing 210009. E-mail: xmren@njut.edu.cn

† Electronic supplementary information (ESI) available: schematic diagram of the topological network, room-temperature excitation spectra, PXRD patterns, TGA curves, and selected bond distances and angles tables of complex **1** and **2**. CCDC reference numbers 792723 and 792724. For ESI and crystallographic data in CIF or other electronic format see DOI: 10.1039/c1dt10693g

two conjugated multicarboxylate ligands, 1,1'-ethynebenzene-3,3',5,5'-tetracarboxylate (EBTC⁴⁻) and 1,1'-butadiynebenzene-3,3',5,5'-tetracarboxylate (BBTC⁴⁻) (Scheme 1), as the "antenna" ligands, and further solvothermal synthesized two EuMOFs with a formula of [Eu₂(EBTC)(DMF)₅(NO₃)₂].DMF (**1**) and [Eu₂(BBTC)_{1.5}(CH₃OH)₂(H₂O)₂].7DMF.HNO₃ (**2**) and studied their characteristic fluorescence from the Eu³⁺ ion.



Scheme 1 Illustration for the molecular structures of H₄EBTC and H₄BBTC.

Herein we present the solvothermal syntheses, crystal structures, photophysical and magnetic properties for the two novel Eu³⁺ coordination polymers.

Experimental

General

All commercially available chemicals were of analytical grade and used as received without further purification. 1,1'-Ethynebenzene-3,3',5,5'-tetracarboxylic acid (H₄EBTC) is prepared according to the method published before,⁷ and 1,1'-butadiynebenzene-3,3',5,5'-tetracarboxylic acid (H₄BBTC) is synthesized by a modified method according to the literature.⁸ Elemental analyses (C, H and N) were carried out on a Perkin-Elmer 240 analyzer. The FTIR spectra were obtained on a VECTOR TM 22 spectrometer with KBr pellets in the 400–4000 cm⁻¹ region. The absorption spectra were obtained from a Shimadzu UV-3100 spectrometer. The MS spectra were measured on a Bruker Daltonics flexAnalysis autoflexTOF/TOF spectrometer using cinnamic acid as a matrix, or on a Finnigan LCQ electron spray mass spectrometer. ¹H and ¹³C NMR spectra were recorded on a Bruker DRX-500 spectrometer at ambient temperature with tetramethylsilane as an internal reference. TGA-DTA diagrams were recorded by a CA Instruments DTA-TGA 2960 type simultaneous analyzer heating from 293 to 1073 K in nitrogen atmosphere at a rate of 20 K min⁻¹. Powder X-ray diffraction (PXRD) data were recorded on a Shimadzu XRD-6000 diffractometer with Cu-Kα (λ = 1.54056 Å) radiation at room temperature with a scan speed of 5° min⁻¹ and a step size of 0.02° in 2θ. Photoluminescence spectra in the solid state were recorded with a Hitachi 850 fluorescence spectrophotometer. The photoluminescence lifetime was measured with an Edinburgh Instruments FLS920P fluorescence spectrometer. Temperature-dependent magnetic susceptibility measurements were performed on a Quantum Design MPMS-XL7 SQUID magnetometer under an applied field of 100 Oe over a temperature range of 1.8–300 K.

Preparations

Tetramethyl 1,1'-butadiynebenzene-3,3',5,5'-tetracarboxylate. Anhydrous Et₃N (20 ml) and tetrahydrofuran (20 ml) were added to a flask containing a mixture of dimethyl 5-ethynylisophthalate⁷ (4.2 g, 19 mmol), Pd(PPh₃)₂Cl₂ (0.2710 g, 0.3861 mmol) and cuprous chloride (0.0764 g, 0.772 mmol). The resulting mixture was heated at 50 °C for 24 h during which oxygen was bubbled into the solution. The solvent was removed *in vacuo* and the residue was extracted with dichloromethane and saturated ammonium chloride solution, and dried over anhydrous MgSO₄. After filtration and evaporation, flash column chromatography on silica gel using dichloromethane as eluant gave the product. Yield 2.9 g (34.7%). Anal. Calcd. For C₂₄H₁₈O₈: C, 66.36; H, 4.18. Found: C, 66.34; H, 4.04. IR (KBr disc, cm⁻¹): 3423 (br), 2950 (w), 1728 (s), 1330 (m), 1245 (s), 1001 (m), 752 (m). ¹H NMR (300 MHz, CDCl₃): δ 3.97 (s, 12H, CH₃), 8.37 (s, 4H, ArH), 8.67 (s, 2H, ArH). ¹³C NMR (500 MHz, CDCl₃): δ 52.6 (CH₃), 137.3, 130.0, 128.8, 122.5 (Ar), 77.4, 75.1 (C≡C), 165.2 (C=O). MS: *m/z* 433.90 (calcd 434.10).

1,1'-Butadiynebenzene-3,3',5,5'-tetracarboxylic acid (H₄BBTC). To a stirred solution of tetramethyl 1,1'-butadiynebenzene-3,3',5,5'-tetracarboxylate (0.2 g) in methanol/water (*V*: *V* = 9: 1, 6.0 ml), potassium hydroxide (0.42 g) was added and the mixture was heated at 80 °C for 24 h, then acidified with 6 M hydrochloric acid. The precipitate was removed by filtration, washed with water for several times, and dried *in vacuo*. Yield 0.15 g (85%). Anal. Calcd. for C₂₀H₁₀O₈: C, 63.50; H, 2.66. Found: C, 63.84; H, 2.93. IR (KBr disc, cm⁻¹): 3415 (br), 3083 (w), 2360 (w), 1707 (s), 1446 (m), 1277 (m), 918 (w), 759 (w). MS: *m/z* 377.50 [M-1]⁻ (calcd 377.30).

[Eu₂(EBTC)(DMF)₅(NO₃)₂].DMF (1**).** The mixture of 1,1'-butadiynebenzene-3,3',5,5'-tetracarboxylic acid (H₄EBTC, 5.0 mg), Eu(NO₃)₃·*n*H₂O (14 mg), DMF (0.4 ml), methanol (two drops) and HNO₃ (0.06 ml, 1 M in DMF) was heated at 85 °C for 12 h. After being slowly cooled to room temperature, colorless block-shaped crystals were achieved (0.30 g, *ca.* 56% based on H₄EBTC). Anal. Calcd for C₃₆H₄₈Eu₂N₈O₂₀: C: 35.44; H: 3.98; N: 9.16; Found: C: 35.50; H: 3.94; N: 9.20. IR (KBr disc, cm⁻¹): 3390 (br), 3062 (w), 2931 (w), 1656 (s), 1433 (s), 1381 (s), 1299 (s), 1107 (m), 786 (m), 717 (m), 673 (m).

[Eu₂(BBTC)_{1.5}(CH₃OH)₂(H₂O)₂].7DMF.HNO₃ (2**).** Sandy beige polyhedral crystals were grown from a solution of 1,1'-butadiynebenzene-3,3',5,5'-tetracarboxylic acid (H₄BBTC, 5.0 mg), Eu(NO₃)₃·*n*H₂O (13 mg), DMF (0.4 ml), methanol (two drops) and HNO₃ (0.03 ml, 1 M in DMF) at 85 °C for 17 h (0.23 g, 86% based on H₄BBTC). Anal. Calcd for C₅₃H₇₁Eu₂N₈O₂₆: C: 40.33; H: 4.65; N: 7.28; Found: C: 40.78; H: 4.24; N: 7.00. IR (KBr disc, cm⁻¹): 3395 (br), 2928 (w), 1657 (s), 1433 (s), 1380 (s), 1103 (m), 780 (m), 717 (m), 672 (m).

Crystallographic analyses

Single crystal X-ray diffraction data were collected on a Bruker Smart Apex II CCD diffractometer at 291 K using graphite monochromated Mo/Kα radiation (λ = 0.71073 Å). The coordinates of the non-hydrogen atoms were refined anisotropically, and all hydrogen atoms were put in calculated positions and refined

Table 1 Crystallographic data and structural refinements for complex **1** and **2**

Complex	1	2 ^b
Empirical formula	C ₃₆ H ₄₈ Eu ₂ N ₈ O ₂₀	C ₃₂ H ₂₁ Eu ₂ O ₁₆
Formula weight	1216.76	965.43
<i>T</i> /K	291(2)	291(2)
Wavelength (Å)	0.71073	0.71073
Crystal size /mm	0.19 × 0.17 × 0.14	0.20 × 0.18 × 0.15
Crystal system	Monoclinic	Monoclinic
Space group	<i>P</i> 2 ₁ / <i>c</i>	<i>C</i> 2/ <i>c</i>
<i>a</i> /Å	13.989(3)	30.208(5)
<i>b</i> /Å	16.567(3)	21.295(5)
<i>c</i> /Å	21.933(3)	18.632(3)
β /°	110.731(10)	94.434(5)
<i>V</i> /Å ³	4754.0(15)	11950(4)
<i>Z</i>	4	8
<i>F</i> (000)	2424	3736
$\theta_{\text{min,max}}$ /°	1.96–26.00	1.91–26.00
GOF	1.004	0.871
<i>R</i> ₁ , <i>wR</i> ₂ [<i>I</i> > 2σ(<i>I</i>)] ^a	0.0577, 0.1250	0.0668, 0.1681

^a $R = \sum ||F_o| - |F_c|| / \sum |F_o|$; $wR_2 = \{ \sum [w(F_o^2 - F_c^2)^2] / \sum (w(F_o^2))^2 \}^{1/2}$. ^b The contribution of solvent electron density was removed by SQUEEZE in its crystallographic data.

isotropically, with the isotropic vibration parameters related to the non-hydrogen atom to which they are bonded. In complex **2**, solvent molecules in the structure were highly disordered and were impossible to refine using conventional discrete-atom models. To resolve this issue, the contribution of solvent electron density was removed by SQUEEZE routine in PLATON.⁹ The main data of collection and refinement details of complexes **1** and **2** are given in Table 1. Selected bond lengths and angles are listed in Table S1 and Table S2 (ESI[†]).

Result and discussion

Syntheses

Ligand 1,1'-ethynebenzene-3,3',5,5'-tetracarboxylic acid (H₄E-BTC) was prepared according to the published procedure in the literature.⁷ 1,1'-Butadiynebenzene-3,3',5,5'-tetracarboxylic acid (H₄BBTC) was hydrolyzed from tetramethyl 1,1'-butadiynebenzene-3,3',5,5'-tetracarboxylate, which is obtained from oxidative alkyne homocoupling of dimethyl 5-ethynylisophthalate catalyzed by a combination of copper and palladium salts.^{8c} Complexes **1** and **2** obtained as crystals were grown under similar solvothermal conditions from a solution of the corresponding tetracarboxylate ligand and Eu(NO₃)₃ in a mixed solvent of DMF, methanol and HNO₃ (1 M in DMF) at the same temperature of 85 °C. It is interesting that the two complexes exhibit quite different crystal structures. **1** has a 2-D layered motif, while **2** displays a 3-D microporous network. This structural distinction may be mainly due to the different rigidity of the two ligands. Compared with EBTC⁴⁻, BBTC⁴⁻ is more flexible since the butadiyne group can make the two aromatic rings rotate more freely than those linked by the ethyne group. As a result, the butadiyne group in BBTC⁴⁻ is bent to a different degree, with one-half of the aromatic rings of the ligands rotated round the butadiyne group to be almost perpendicularly arranged in order to satisfy the coordination geometry of Eu³⁺. Moreover, the larger center of lanthanide Eu³⁺ also plays an important

role for the structural construction. It has been reported that 3-D cupric microporous paddle-wheel MOFs were generated not only for H₄BBTC,¹⁰ but also for H₄EBTC.^{7,11} Since lanthanides have larger coordination spheres and more flexible coordination geometries compared with the first-row transition metals,¹² they need more coordination donors with larger space. Thus, besides ligands of EBTC⁴⁻ or BBTC⁴⁻, not only water, but also some other bulky molecules or anions, such as DMF, methanol and NO₃⁻, coordinate to Eu³⁺, leading to completely different structures detailed below.

Structure description

Structure of [Eu₂(EBTC)(DMF)₅(NO₃)₂].DMF (1**).** Crystal of **1** belongs to the monoclinic space group *P*2₁/*c*, with its asymmetric unit consisting of two different Eu³⁺ ions, one deprotonated EBTC⁴⁻ ligand, five coordinated DMF molecules, two coordinated NO₃⁻ anions and one guest DMF molecule. As shown in Fig. 1, the two crystallographically independent Eu³⁺ ions exhibit different coordination geometries. The Eu1 ion is nine-coordinated to form a distorted monocapped square-antiprism coordination geometry, in which four oxygen atoms (O2, O5c, O7b and O8b) come from one EBTC⁴⁻ ligand, four oxygen atoms (O9, O10, O12 and O13) from two NO₃⁻ anions, and one (O15) from a DMF molecule to result in a [Eu1O₉] unit. The Eu2 ion is eight-coordinated with a [Eu2O₈] unit, which adopts a distorted square-antiprism coordination geometry bonding to four oxygen donors (O1a, O6b, O3 and O4) from one EBTC⁴⁻ ligand and another four (O16, O17, O18 and O19) from four DMF molecules. The Eu–O bond lengths vary from 2.303 to 2.534 Å, which are in the ranges compatible with the values of the previously published lanthanide complexes with carboxylic acids as bridging ligands.¹³

As illustrated in Fig. 2, four carboxylates of the EBTC⁴⁻ ligand coordinate to the Eu³⁺ ions *via* two types of coordination modes: two carboxylates in the *trans*-direction adopt a bidentate bridging mode to connect two Eu1 and two Eu2 centers with an Eu1...Eu2 distance of 5.714 Å, and the other two, also in the *trans*-direction, adopt a chelating mode to coordinate one Eu1 and one Eu2 center, respectively. Therefore, each EBTC⁴⁻ ligand links three Eu1 and three Eu2 ions to generate a binuclear Eu1Eu2(CO₂)₄ subunit. As a result, each binuclear subunit bridges four EBTC⁴⁻ ligands and each EBTC⁴⁻ ligand connects four binuclear subunits to form a ladder-like architecture plane along the crystallographic *b*-axis direction. Weak intramolecular hydrogen-bonding interactions (C25A—H25A...O4, with a hydrogen bond distance of 3.00(2) Å and an angle of 122.00°) exist between coordinated DMF and EBTC⁴⁻ ligands. Solvent DMF molecules, as well as the coordinated DMF molecules and NO₃⁻ anions, exist within the adjacent ladder-like 2-D layers, leading to 3-D supramolecular structure formation due to the Van der Waals force interactions. Furthermore, it is worth noting that EBTC⁴⁻ almost keeps its coplanarity and the ethyne group retains its linearity upon coordination. The dihedral angle between the two aromatic rings in **1** is 5.875°, and the bond angles in the C_{Ar}—C≡C—C_{Ar} moiety are 175.76° (C8–C9–C10) and 177.36° (C9–C10–C11), respectively.

From a topological perspective, taking the center of the aryl rings as 3-connected nodes and the center of the binuclear as four connected nodes, a trinodal (3, 4)-connected network was schematically represented in Fig. S1 (ESI[†]) with the overall Schläfli symbol of (4.6)₂(4².6².8²).

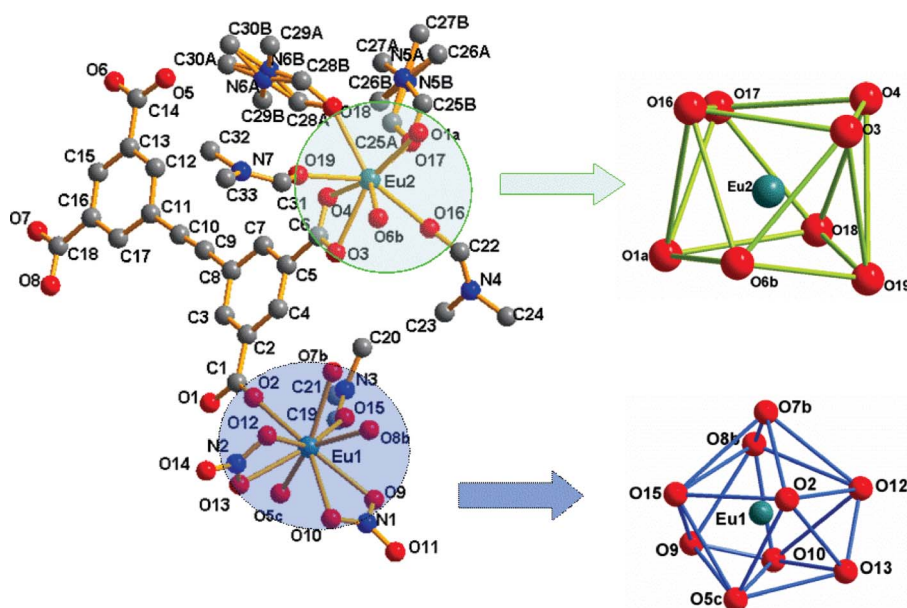


Fig. 1 The local coordination environment of Eu1 and Eu2 ions in **1** with the H atoms omitted for clarity. Color scheme: Eu: teal; O: red; N: blue; C, gray. Symmetry codes: $a = x, 1.5 - y, 0.5 + z$; $b = 1 + x, 1.5 - y, 0.5 + z$; $c = 1 + x, y, z$.

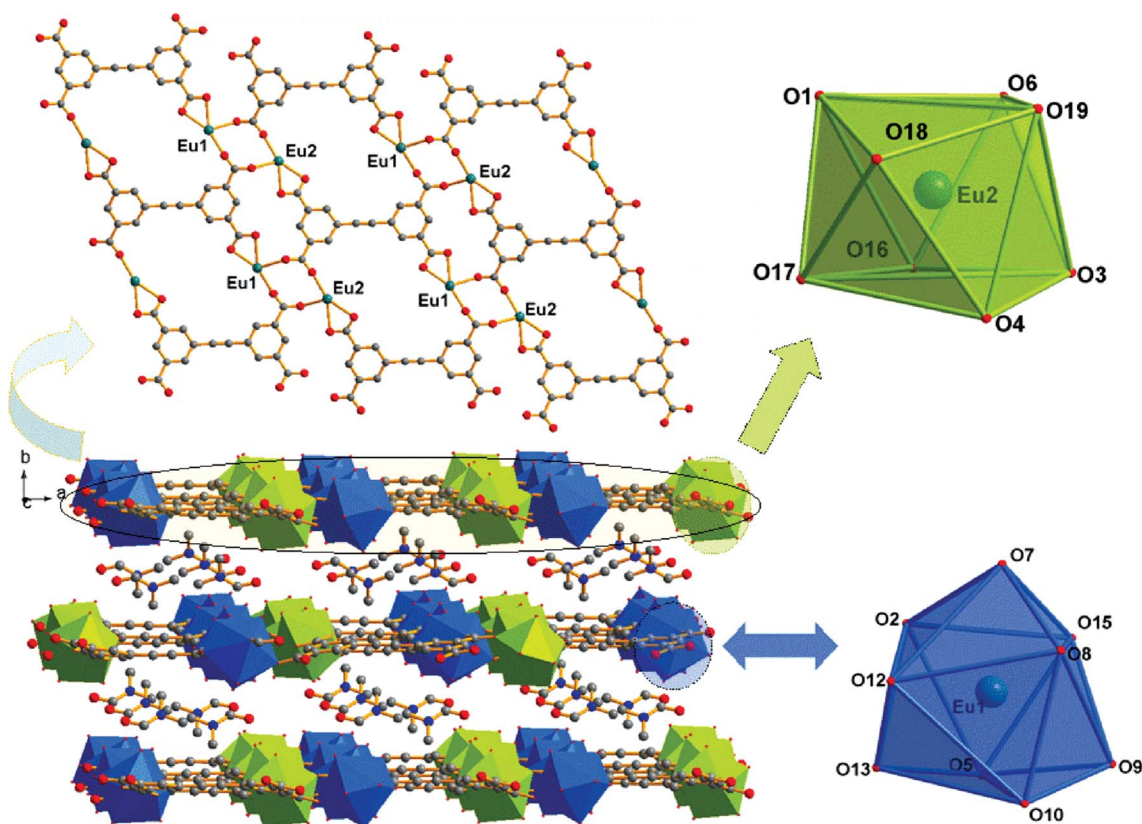


Fig. 2 Perspective view of the 2-D layers in the ab plane. Light blue polyhedra represent Eu1 ions, and lime polyhedra represent Eu2 ions. Hydrogens, coordinated DMF molecules and NO_3^- anions are omitted for clarity.

Structure of $[\text{Eu}_2(\text{BBTC})_{1.5}(\text{CH}_3\text{OH})_2(\text{H}_2\text{O})_2] \cdot 7\text{DMF} \cdot \text{HNO}_3$ (2**).** Crystal **2** crystallizes in the monoclinic system with a space group of $C2/c$. Its asymmetric unit cell contains two crystallographically unique Eu^{3+} ions, one and a half BBTC^{4-} , two coordinated water molecules and two coordinated methanol molecules.

As shown in Fig. 3a, two crystallographically independent Eu^{3+} ions exhibit different coordination geometries in **2** although both of them are coordinated by eight oxygen atoms. Eu1 displays distorted square-antiprism coordination geometry with its eight coordinated oxygen atoms coming from five BBTC^{4-} ligands

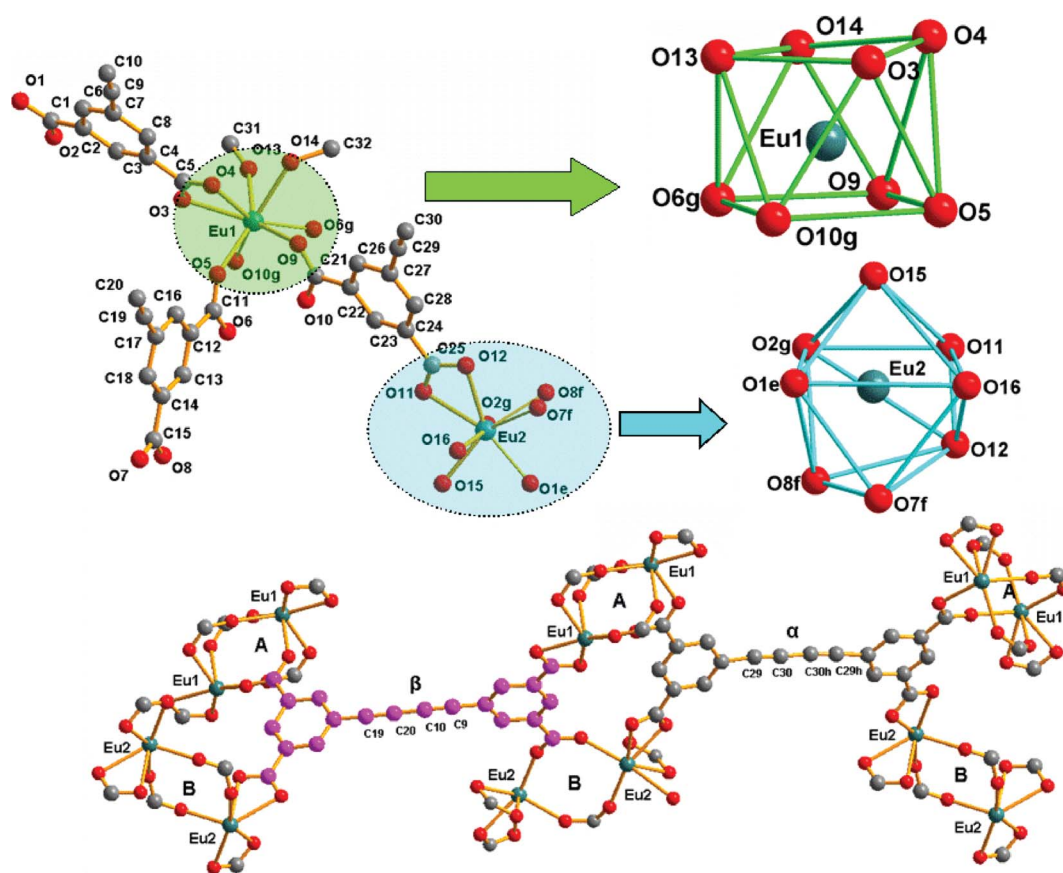


Fig. 3 (a) The asymmetric unit of **2** with the H atoms omitted for clarity. Color scheme: Eu, teal; O, red; C, gray. Symmetry codes: $e = x, 1 + y, z; f = x, 2 - y, 0.5 + z; g = 1.5 - x, 1.5 - y, 1 - z; h = 2 - x, y, 1.5 - z$. (b) The local coordination environment of the Eu1 and Eu2 ions in **2**. A and B represent $\text{Eu}_2(\text{CO}_2)_4$ and $\text{Eu}_2(\text{CO}_2)_2$ subunits, respectively; α and β represent BBTC^+ ligands with two different steric forms.

(O3, O4, O5, O6g, O9 and O10g) and two methanol molecules (O13, O14). Among the five coordinated BBTC^+ ligands, one carboxylate from one BBTC^+ coordinates to Eu1 as a chelating mode, while the other four carboxylates from four different BBTC^+ ligands coordinate to two Eu1 centers in a bidentate bridging coordination mode to result in an irregular paddle-wheel binuclear $\text{Eu}_2(\text{CO}_2)_4$ (A) unit, with $\text{Eu1} \cdots \text{Eu1}$ distance of 4.275 Å. As for Eu2, it adopts a trigondodecahedron coordination mode, which bonds to six oxygen donors (O1e, O2g, O7f, O8f, O11 and O12) from four BBTC^+ ligands, and the two remnant sites (O15, O16) are occupied by two water molecules. Similarly, two Eu2 centers are linked by two carboxylates in a bidentate bridging coordination mode from two different BBTC^+ ligands to form a binuclear $\text{Eu}_2(\text{CO}_2)_2$ (B) subunit, with $\text{Eu2} \cdots \text{Eu2}$ distance of 5.360 Å. Furthermore, two more carboxylates from another two BBTC^+ ligands coordinate to Eu2 as chelating mode. Eventually, two kinds of BBTC^+ ligand (α and β) with different steric configurations generate upon complexation as shown in Fig. 3b. The torsion angle of the butadiyne group (C29-C30-C30h-C29h) is 150.973° and the dihedral angle between the two aromatic rings is 8.708° in α form, while those in β form are 14.073° (C9-C10-C20-C19) and 87.340°, respectively. That is to say, the butadiyne group would bend more in order to keep the coplanarity of the two aromatic rings in BBTC^+ ligand, or the two aromatic rings would rotate to nearly perpendicular direction. In the α - BBTC^+ ligand,

two carboxylates in the *cis*-positions adopt bidentate mode to bridge two Eu1 centers, and the other two adopt chelating mode to bind two Eu2 atoms. In the β - BBTC^+ ligand, two opposite carboxylates in two phenyl rings adopt a bidentate bridging mode to link two Eu1 and two Eu2 centers, and the other two also in opposite positions adopt a chelating mode to coordinate Eu1 and Eu2 center, respectively. Overall, each BBTC^+ ligand connects two $\text{Eu}_2(\text{CO}_2)_4$ (A) units and two $\text{Eu}_2(\text{CO}_2)_2$ (B) blocks. The bond lengths of Eu–O vary from 2.300 to 2.714 Å, which are within the range of those usually encountered for lanthanide oxygen coordination.

Since the organic BBTC^+ building units and the inorganic $\text{Eu}_2(\text{CO}_2)_4$ (A) and $\text{Eu}_2(\text{CO}_2)_2$ (B) building blocks in **2** are alternately linked to each other, a 3-D porous metal-organic framework is eventually constructed. As shown in Fig. 4, there exist three types of one-dimensional channels along the *c* axis, which possesses the open window of 4.3×1.8 Å (D), 4.8×2.5 Å (E) and 5.9×2.3 Å (F), respectively. Moreover, open channel systems also exist along the *a* and *b* axis, with an open window size of 5.6×5.6 Å and 5.8×2.5 Å, respectively. The accessible pore volume from the single crystal structure is 53.4%, as calculated using the Platon program.¹⁴ When the coordinated methanol and water molecules are removed, the volume increases up to 61.8%.

A better insight into this framework can be achieved by topology analysis. With regard to the connectivity describing above, the

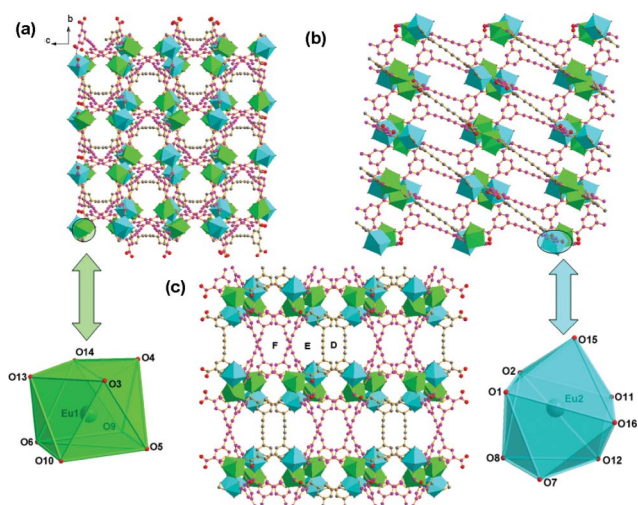


Fig. 4 Polyhedral representation of **2** seen from *a*, *b*, and *c* directions (the green and turquoise polyhedra correspond to $[\text{Eu}1\text{O}_8]$ and $[\text{Eu}2\text{O}_8]$ units, respectively).

center of the $\text{Eu}_2(\text{CO}_2)_4$ (A) and $\text{Eu}_2(\text{CO}_2)_2$ (B) units can be considered as six-connected nodes, and the aryl rings can be viewed as three-connected nodes. As a result, a (3,6)-connected net with a Schläfli point symbol of $(4.6^2)_2(4^2.6^6.8^8.10)$ is obtained for compound **2** (Fig. S2, ESI†).

UV-vis spectra analyses

The absorption spectra of complexes **1** and **2**, together with the ligands of H_4EBTC and H_4BBTC in the solid state, are shown in Fig. 5 and Fig. S6†, respectively. The ligands H_4EBTC and H_4BBTC exhibit absorptions with intense and sharp bands at *ca.* 300 nm and 298, 318, 346 nm, respectively, which can be assigned to the $\pi-\pi^*$ transitions. Similar absorption bands are observed in complex **1** (289 and 309 nm) and complex **2** (297, 316 and 339 nm). These bands are also probably due to the $\pi-\pi^*$ transitions of the ligands. It is obvious that the $\pi-\pi^*$ transitions of complex **2** and ligand H_4BBTC are bathochromically shifted compared with those of complex **1** and ligand H_4EBTC , respectively, which is due to a larger π -conjugative effect in compound **2** and H_4BBTC .

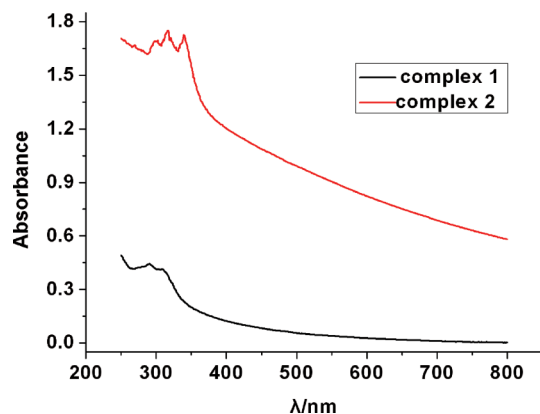


Fig. 5 UV-vis spectra of complex **1** and **2**.

Photophysical properties

The emission spectra upon excitation at 397 nm for **1** and 340 nm for **2** are displayed in Fig. 6, from which the characteristic intense red luminescence originating from f-f transitions of the Eu^{3+} ion are observed. The emission bands centered at 581, 595, 620, 652, 703 nm for **1** versus 580, 593, 615, 652, 695 nm for **2** correspond to $^5\text{D}_0 \rightarrow ^7\text{F}_n$ ($n = 0 \rightarrow 4$) transition of Eu^{3+} ions, respectively. Among them, the symmetric forbidden emission $^5\text{D}_0 \rightarrow ^7\text{F}_0$ around 580 nm is almost invisible, the medium-strong emission around 590 nm is attributed to the magnetic-dipolar $^5\text{D}_0 \rightarrow ^7\text{F}_1$ transition, and the most intense emission around 620 nm is ascribed to the electric-dipolar $^5\text{D}_0 \rightarrow ^7\text{F}_2$ transition.¹⁶ Moreover, the weak emission peaks round 650 nm ($^5\text{D}_0 \rightarrow ^7\text{F}_3$) and 700 nm ($^5\text{D}_0 \rightarrow ^7\text{F}_4$) also correspond to the magnetic dipole transitions.¹⁷ Since the electric-dipolar $^5\text{D}_0 \rightarrow ^7\text{F}_2$ transition is hypersensitive to the coordination environment of the Eu^{3+} ions, while the magnetic-dipolar $^5\text{D}_0 \rightarrow ^7\text{F}_1$ transition is fairly insensitive to it, the much stronger intensity of the $^5\text{D}_0 \rightarrow ^7\text{F}_2$ transition in these complexes (the intensity ratio of $I(^5\text{D}_0 \rightarrow ^7\text{F}_2) : I(^5\text{D}_0 \rightarrow ^7\text{F}_1)$ is 5.50 and 4.33 for **1** and **2**, respectively) indicates that the Eu^{3+} ion adopts a noncentrosymmetric coordination environment without an inversion center,¹⁸ which is in good agreement with the result of single-crystal X-ray analysis.

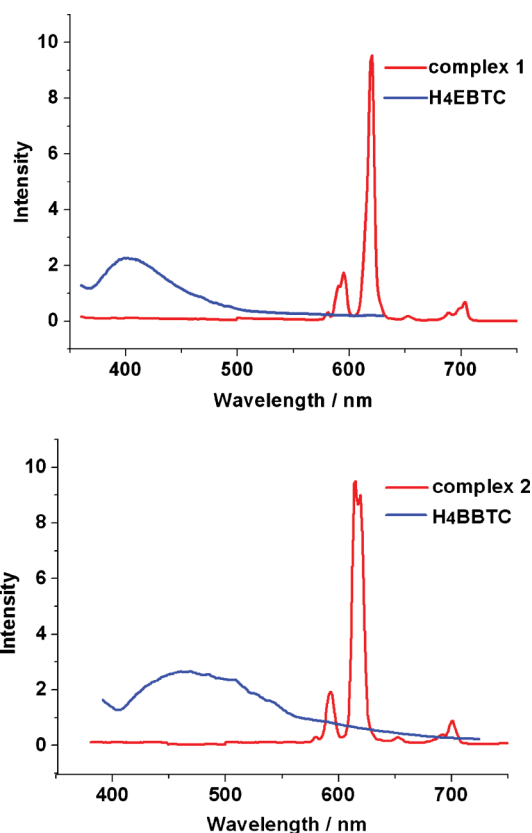


Fig. 6 Emission spectra of **1** (a) and **2** (b) in the solid state at ambient temperature.

As shown in Fig. 6, the π -conjugated ligands in the compounds H_4EBTC and H_4BBTC display broad fluorescent emission bands centered at 402 and 453 nm upon excitation at 342 and 396 nm in the solid state at room temperature, respectively, and these

emission bands arise from the intramolecular $\pi-\pi^*$ transition of the corresponding ligands. In comparison to the fluorescence spectra of **1**, **2** and H₄EBTC, H₄BBTC, the disappearance of intramolecular $\pi-\pi^*$ transition of ligands in the corresponding Eu³⁺ coordination polymers indicates that an efficient energy transfer process occurs from the conjugated tetracarboxylate ligands to Eu³⁺ ions in **1** and **2**. The energy transfer process between the ligand and the Eu³⁺ ions can be described as below: the EBTC⁴⁻/BBTC⁴⁻ ligand absorbs energy from external source into S₁ from its S₀, then proceeds on the internal conversion to T₁ from the lowest vibration level of S₁ and further proceeds to an intramolecular energy transfer from T₁ of the ligand to the localized ⁵D₀ energy level of the central Eu³⁺ ion, which emits multiple characteristic emissions of the Eu³⁺ ion from ⁵D₀ → ⁷F_J.¹⁵

The fluorescence lifetime, τ , of the two complexes are investigated in the solid state at room temperature, and the curves of the fluorescence decay of **1** and **2** are illustrated in Fig. 7. The process of fluorescence decay for both **1** and **2** follows a single exponential decay law, as a result, the equation $I_t = A_0 + A_1 \times \exp(-t/\tau)$ was utilized for fitting the fluorescence decay curves of **1** and **2**, which gave the best parameters as $A_0 = 0.02534$, $A_1 = 3.35459$ and $\tau = 1.308$ ms with an overall χ^2 of 0.99847, for **1** versus $A_0 = 0.03528$, $A_1 = 3.33493$ and $\tau = 0.702$ ms with an overall χ^2 of 0.9983 for **2**. The f-f electronic transitions of lanthanide are forbidden, leading to long excited state decay time. It was found that the fluorescence lifetimes of **1** and **2** are of millisecond order, falling in the range of lanthanide ion fluorescence decay times of 10–2000 μ s.

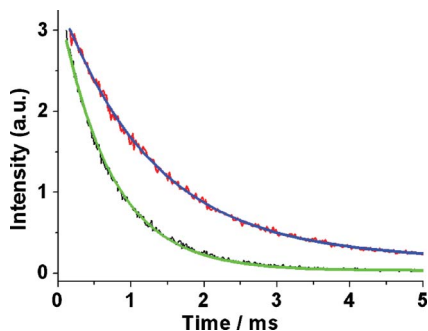


Fig. 7 Typical luminescence decay profile observed for **1** (black) and **2** (red) in the solid state at room temperature, and the green and blue lines are the corresponding monoexponential fits of **1** and **2**, respectively.

Magnetic properties

The variable-temperature magnetic susceptibilities were measured at an applied magnetic field of 100 Oe in the temperature range of 1.8–300 K for **1** and **2** (Fig. 8). The $\chi_M T$ values are 2.5 cm³ K mol⁻¹ for **1** and 3.0 cm³ K mol⁻¹ for **2**, respectively, accounting for the two Eu³⁺ ions. In the whole temperature range, as the temperature decreases, the $\chi_M T$ values gradually decrease and reach nearly zero at 1.8 K, indicating that the f electrons of the Eu³⁺ ions depopulate from their magnetic excited states and populate the diamagnetic ground state of ⁷F₀ during the cooling process.¹⁹

Since the 4f electrons of rare earth ions are shielded by the outer sphere s and p electrons, the superexchange interactions between the rare earth ions are usually very weak. Moreover, by comparing the curves of χ_M and $\chi_M T$ with those of Eu³⁺ mononuclear complexes, it is interesting to find that they are very

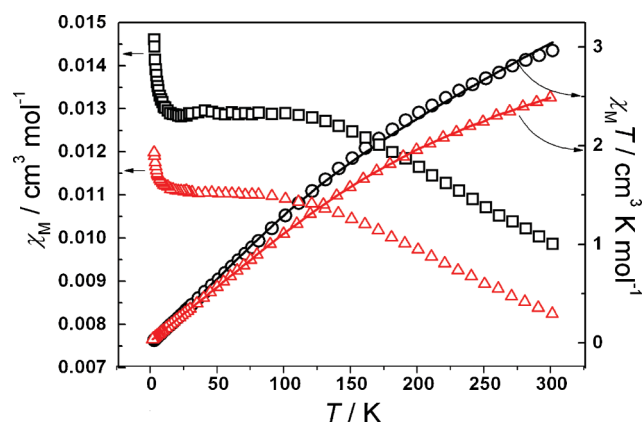


Fig. 8 Temperature dependence of χ_M and $\chi_M T$ for **1** (red) and **2** (black).

similar.²⁰ Thus, the magnetic susceptibilities of **1** and **2** can be fitted with a single-ion Eu³⁺ model based on eqn (1),²¹ which only considers the spin-orbital coupling of Eu³⁺ ions.

$$\chi_M = \frac{N\beta^2 A}{3kTx} + TIP$$

$$A = 24 + \left(\frac{27x}{2} - \frac{3}{2}\right)e^{-x} + \left(\frac{135x}{2} - \frac{5}{2}\right)e^{-3x} + \left(189x - \frac{7}{2}\right)e^{-6x} + \left(405x - \frac{9}{2}\right)e^{-10x} + \left(\frac{1458x}{2} - \frac{11}{2}\right)e^{-15x} + \left(\frac{2457x}{2} + \frac{13}{2}\right)e^{-21x}$$

$$B = 1 + 3e^{-x} + 5e^{-3x} + 7e^{-6x} + 9e^{-10x} + 11e^{-15x} + 13e^{-21x}$$

where $x = \lambda/kT$, with λ being the spin-orbital coupling parameter, k being the Boltzmann constant and TIP being the temperature independent magnetism. Through fitting the $\chi_M T$ vs. T plots of the whole temperature range, the best fitting results are $\lambda = 265$ cm⁻¹ and $TIP = 3.31 \times 10^{-3}$ with $R = \Sigma[(\chi_M T)_{\text{calc}} - (\chi_M T)_{\text{obsd}}]^2 / \Sigma[(\chi_M T)_{\text{obsd}}]^2 = 1.7 \times 10^{-4}$ for **1**, and $\lambda = 251$ cm⁻¹ and $TIP = 4.95 \times 10^{-3}$ with an agreement factor R of 6.9×10^{-4} for **2**. The λ parameters are in good agreement with the literature values.²² The analyses for the magnetic behaviors of **1** and **2** demonstrate that the Eu³⁺ ions are well isolated from each other in the magnetic molecule field, even if the distances between the Eu³⁺ ions are rather short.

Conclusion

Two Eu³⁺ coordination polymers, based on the conjugated tetracarboxylate ligands of EBTC⁴⁻ and BBTC⁴⁻, were successfully synthesized under similar hydrothermal conditions. Coordination compound **1** has a 2-D layered structure with a binuclear Eu₁Eu₂(CO₂)₄ subunit linked by EBTC⁴⁻, while **2** exhibits a 3-D microporous network containing two different subunits of Eu₂(CO₂)₄ and Eu₂(CO₂)₂ connected by BBTC⁴⁻. The structural differences are probably caused by the flexibility/rigidity of the ligand and the diverse metal center matched by different coordination geometry. **1** and **2** display single-ion Eu³⁺ magnetic behaviors. Moreover, they intensely emit the characteristic red luminescence of the Eu³⁺ ion with a long lifetime (1.3 ms for **1** and 0.7 ms for **2**) under ultraviolet excitation at room temperature. Meanwhile, the emission bands originating from the intramolecular $\pi^* \rightarrow \pi$ transition of the ligand disappeared, which indicate the existence of efficient energy transfer from the conjugated tetracarboxylate

ligands to the Eu^{3+} ions. Therefore, the $\text{EBTC}^+/\text{BBTC}^+$ ligands are effective “antenna” ligands for the luminescent Eu^{3+} ion. This work provides helpful information for the design and construction of highly luminescent Ln-based coordination polymers, which have potential applications in optical and electrooptical devices as well as time-resolved fluorescence assays.

Acknowledgements

This work was supported by the Major State Basic Research Development Program (Grant 2007CB925103) and the Nature Science Foundation of China (Grant 20871068).

References

- (a) R. D. Archer, H. Chen and L. C. Thompson, *Inorg. Chem.*, 1998, **37**, 2089; (b) M. Hernández-Molina, C. Ruiz-Pérez, T. López, F. Lloret and M. Julve, *Inorg. Chem.*, 2003, **42**, 5456; (c) C. Serre, F. Millange, C. Thouvenot, N. Gardant, F. Pellé and G. Férey, *J. Mater. Chem.*, 2004, **14**, 1540; (d) B. L. Chen, Y. Yang, F. Zapata, G. D. Qian, Y. S. Luo, J. H. Zhang and E. B. Lobkovsky, *Inorg. Chem.*, 2006, **45**, 8882; (e) Z. Chen, B. Zhao, Y. Zhang, W. Shi and P. Cheng, *Cryst. Growth Des.*, 2008, **8**, 2291; (f) G. J. He, D. Guo, C. He, X. L. Zhang, X. W. Zhao and C. Y. Duan, *Angew. Chem., Int. Ed.*, 2009, **48**, 6132.
- (a) T. Sanada, T. Suzuki, T. Yoshida and S. Kaizaki, *Inorg. Chem.*, 1998, **37**, 4712; (b) R. E. P. Winpenny, *Chem. Soc. Rev.*, 1998, **27**, 447; (c) J. P. Costes, A. Dupuis and J. P. Laurent, *J. Chem. Soc., Dalton Trans.*, 1998, 735; (d) T. K. Maji, G. Mostafa, H. C. Chang and S. Kitagawa, *Chem. Commun.*, 2005, 2436; (e) D. Aguilà, L. A. Barrios, F. Luis, A. Repollés, O. Roubeau, S. J. Teat and G. Aromí, *Inorg. Chem.*, 2010, **49**, 6784.
- (a) J. C. G. Bünzli and C. Piguet, *Chem. Soc. Rev.*, 2005, **34**, 1048; (b) R. J. Hill, D. L. Long, P. Hubberstey, M. Schroder and N. R. Champness, *J. Solid State Chem.*, 2005, **178**, 2414; (c) K. L. Wong, G. L. Law, Y. Y. Yang and W. T. Wong, *Adv. Mater.*, 2006, **18**, 1051; (d) C. L. Cahill, D. T. de Lill and M. Frisch, *CrystEngComm*, 2007, **9**, 15; (e) C. Marchal, Y. Filinchuk, D. Imbert, J. C. G. Bünzli and M. Mazzanti, *Inorg. Chem.*, 2007, **46**, 6242.
- (a) N. Sabbatini, M. Guardigli and J. M. Lehn, *Coord. Chem. Rev.*, 1993, **123**, 201; (b) Allendorf, C. A. Bauer, R. K. Bhakta and R. J. T. Houk, *Chem. Soc. Rev.*, 2009, **38**, 1330.
- Z. J. Lin, B. Xu, T. F. Liu, M. N. Cao, J. Lü and R. Cao, *Eur. J. Inorg. Chem.*, 2010, **24**, 3842.
- J. Rocha, L. D. Carlos, F. A. A. Paz and D. Ananias, *Chem. Soc. Rev.*, 2011, **40**, 926.
- Y. X. Hu, S. C. Xiang, W. W. Zhang, Z. X. Zhang, L. Wang, J. F. Bai and B. L. Chen, *Chem. Commun.*, 2009, 7551.
- (a) J. T. Lin, S. S. Sun, J. J. Wu, L. Lee, K. J. Lin and Y. F. Huang, *Inorg. Chem.*, 1995, **34**, 2323; (b) M. Maekawa, K. Sugimoto, T. Kurodasowa, Y. Suenaga and M. Munakata, *J. Chem. Soc., Dalton Trans.*, 1999, 4357; (c) K. Kamata, S. Yamaguchi, M. Kotani, K. Yamaguchi and N. Mizuno, *Angew. Chem., Int. Ed.*, 2008, **47**, 2407.
- A. L. Spek, *J. Appl. Crystallogr.*, 2003, **36**, 7.
- (a) D. Zhao, D. Yuan, A. Yakovenko and H. C. Zhou, *Chem. Commun.*, 2010, **46**, 4196; (b) B. Zheng, Z. Liang, G. Li, Q. Huo and Y. Liu, *Cryst. Growth Des.*, 2010, **10**, 3405.
- D. F. Sun, S. Q. Ma, J. M. Simmons, J. R. Li, D. Q. Yuan and H. C. Zhou, *Chem. Commun.*, 2010, **46**, 1329.
- D. J. Tranchemontagne, J. L. Mendoza-Cortes, M. O’Keeffe and O. M. Yaghi, *Chem. Soc. Rev.*, 2009, **38**, 1257.
- (a) P. X. Yin, Z. J. Li, J. Zhang, L. Zhang, Q. P. Lin, Y. Y. Qin and Y. G. Yao, *CrystEngComm*, 2009, **11**, 2734; (b) J. G. Wang, C. C. Huang, X. H. Huang and D. S. Liu, *Cryst. Growth Des.*, 2008, **8**, 795; (c) Y. Q. Sun, J. Zhang and G. Y. Yang, *Chem. Commun.*, 2006, 1947; (d) J. W. Cheng, J. Zhang, S. T. Zheng and G. Y. Yang, *Chem.–Eur. J.*, 2008, **14**, 88; (e) Y. G. Huang, F. L. Jiang, D. Q. Yuan, M. Y. Wu, Q. Gao, W. Wei and M. C. Hong, *J. Solid State Chem.*, 2009, **182**, 215; (f) Y. Li, G. Xu, W. O. Zou, N. S. Wang, F. K. Zheng, M. F. Wu, H. Y. Zeng, G. C. Guo and J. S. Huang, *Inorg. Chem.*, 2008, **47**, 7945; (g) V. Kiritsis, A. Michaelides, S. Skoulika, S. Golhen and L. Ouahab, *Inorg. Chem.*, 1998, **37**, 3407.
- A. L. Spek, *J. Appl. Crystallogr.*, 2003, **36**, 7.
- (a) K. A. Gschneider and L. R. Eyring, *Handbook on the Physics and Chemistry of Rare Earths*, North-Holland Publishing Co, Amsterdam, 1979; (b) N. Sabbatini, M. Guardigli and J. M. Lehn, *Coord. Chem. Rev.*, 1993, **123**, 201.
- F. S. Richardson, *Chem. Rev.*, 1982, **82**, 541.
- S. N. Wang, R. Sun, X. S. Wang, Y. Z. Li, Y. Pan, J. F. Bai, M. Scheer and X. Z. You, *CrystEngComm*, 2007, **9**, 1051.
- (a) J. Yang, Q. Yue, G. D. Li, J. J. Cao, G. H. Li and J. S. Chen, *Inorg. Chem.*, 2006, **45**, 2857; (b) M. L. Sun, J. Zhang, Q. P. Lin, P. X. Yin and Y. G. Yao, *Inorg. Chem.*, 2010, **49**, 9257; (c) J. Li, C. C. Ji, Z. Z. Lu, T. W. Wang, Y. Song, Y. Z. Li, H. G. Zheng, Z. J. Guo and S. R. Batten, *CrystEngComm*, 2010, **12**, 4424.
- Y. H. Wan, L. P. Zhang, L. P. Jin, S. Gao and S. Z. Lu, *Inorg. Chem.*, 2003, **42**, 4985.
- (a) Y. G. Huang, B. L. Wu, D. Q. Yuan, Y. Q. Xu, F.-L. Jiang and M.-C. Hong, *Inorg. Chem.*, 2007, **46**, 1171; (b) C.-M. Liu, M. Xiong, D.-Q. Zhang, M. Du and D.-B. Zhu, *Dalton Trans.*, 2009, 5666; (c) C.-D. Wu, C.-Z. Lu, W.-B. Yang, S.-F. Lu, H.-H. Zhuang and J.-S. Huang, *Eur. J. Inorg. Chem.*, 2002, 797.
- M. Andruh, E. Bakalbassis, O. Kahn, J. C. Trombe and P. Porcher, *Inorg. Chem.*, 1993, **32**, 1616.
- X. J. Wang, Z. M. Cen, Q. L. Ni, X. F. Jiang, H. C. Lian, L. C. Gui, H. H. Zuo and Z. Y. Wang, *Cryst. Growth Des.*, 2010, **10**, 2960.